AAPS PharmSciTech, Vol. 18, No. 1, January 2017 (© 2016)
DOI: 10.1208/s12249-016-0491-5

Research Article

In Vitro-In Vivo Evaluation of Novel Co-spray Dried Rifampicin Phospholipid Lipospheres for Oral Delivery

Charan Singh,[1] L. V. Seshu Kumar Koduri,[1] Tara Datt Bhatt,[2] Sarbjit Singh Jhamb,[3] Vijay Mishra,[3] Manjinder Singh Gill,[2] and Sarasija Suresh[1,4,5]

Received 27 August 2015; accepted 28 January 2016; published online 22 December 2016

Abstract. The objective of this study comprises of developing novel co-spray dried rifampicin phospholipid lipospheres (SDRPL) to investigate its influence on rifampicin solubility and oral bioavailability. Solid-state techniques were employed to characterize the liposphere formulation. SDRPL solubility was determined in distilled water. BACTEC 460TB System was employed to evaluate SDRPL antimycobacterial activity. The oral bioavailability of the lipospheres was evaluated in Sprague Dawley rats. Lipospheres exhibited amorphous, smooth spherical morphology with a significant increase ($p < 0.001$) in solubility of SDRPL (2:1), 350.9 ± 23 *versus* 105.1 ± 12 μg/ml and SDRPL (1:1) 306.4 ± 20 *versus* 105.1 ± 12 μg/ml in comparison to rifampicin (RMP). SDRPL exhibited enhanced activity against *Mycobacterium tuberculosis*, H37Rv strain, with over twofolds less minimum inhibitory concentration (MIC) than the free drug. Lipospheres exhibited higher peak plasma concentration (109.92 ± 25 *versus* 54.31 ± 18 μg/ml), faster T_{max} (two *versus* four hours), and enhanced area under the curve ($AUC_{0-\infty}$) (406.92 ± 18 *versus* 147.72 ± 15 μg h/L) in comparison to pure RMP. Thus, SDRPL represents a promising carrier system exhibiting enhanced antimycobacterial activity and oral bioavailability of rifampicin.

KEY WORDS: antimycobacterial activity; bioavailability; carrier system; lipospheres; *Mycobacterium tuberculosis*; pharmacokinetic; rifampicin; solid state; solubility.

INTRODUCTION

Tuberculosis (TB) is one of the most deadly diseases affecting mankind (1,2). It is caused by bacillus *Mycobacterium tuberculosis* (MTB), a facultative intracellular parasite (3,4). The World Health Organization (WHO) estimates that one-third of the world's population is infected with MTB. According to the WHO global TB report 2014, 1.5 million people died from TB, including 360,000 among people who were HIV-positive (5). Although TB is reported all over the world, the highest estimated number of cases in 2013 occurred in Asia and the African Region of 56 and 29%, respectively. India and China are of the six countries that stand out as having the largest number of incident cases in the previous year. This accounts for 24 and 11% of global cases, respectively.

Rifampicin (RMP) is a frontline drug in anti-TB chemotherapy. It is a lipophillic molecule with poor aqueous solubility. RMP is a borderline class II Biopharmaceutical Classification System (BCS) drug (6–10). In therapy, it is administered with isoniazid, pyrazinamide, and ethambutol for 2 months followed by a combination with isoniazid for further 4 months. Long duration of therapy causes hepatotoxicity, failure of treatment and consequently, leads to development of multidrug-resistant TB. Literature survey revealed that several approaches were reported to enhance the solubility and bioavailability of lipophillic molecules by microparticles (11), solid dispersions (12,13), lipid-based formulation, (14) and cyclodextrin complexes (15).

In the last two decades, lipid-based drug delivery systems have been extensively investigated, particularly to increase the bioavailability of BCS class II and class IV drugs. The success of Sandimmune™ and Neoral™, the lipid-based oral products of cyclosporine A, has further intensified the interest (16). In the lipid-based system, the drug hitherto is dissolved in the lipid excipient(s), thus enhancing the solubility of drugs with dissolution-limiting bioavailability. Phospholipids have been employed for oral delivery of therapeutics. They are biodegradable and biocompatible being the major components of the plasma membrane. Phospholipid-based systems have been developed to increase solubility and enhance dissolution rate and bioavailability of water-insoluble drugs, especially phytopharmaceuticals (17–20). Furthermore, they have been investigated to reduce NSAID-induced gastrointestinal toxicity and hepatotoxicity (21).

[1] Department of Pharmaceutical Technology (Formulation), Mohali, India.
[2] Technology Development Center, Mohali, India.
[3] Common Biological Testing Laboratory, Mohali, India.
[4] National Institute of Pharmaceutical Education and Research (NIPER), Sector 67, S.A.S. Nagar, Mohali, Punjab 160062, India.
[5] To whom correspondence should be addressed. (e-mail: sarasija_s@hotmail.com)

In our previous work, we observed considerable enhancement in the solubility and bioavailability of RMP by preparation of its phospholipid complex using conventional solvent evaporation technique (10), which is a time-consuming and multistep approach. Moreover, there is a clear need of an alternative method for preparation of formulation with lesser time and easy scalability. Spray drying is widely employed in microparticle preparation due to the uniform size distribution of the product and advantages of one-step formulation and drying process (22,23). In a quest for an industrially viable, easily scalable method with a capability of modulating the size and thereby dissolution characteristics, we have developed novel co-spray dried rifampicin phospholipid lipospheres (SDRPL) by spray drying technology. SDRPL displayed enhanced aqueous solubility and bioavailability. Further, it exhibited improved *in vitro* antimycobacterial activity when evaluated by the BACTEC 460TB System. Thus, this strategy is easily scalable and has the potential for oral delivery of lipospheres.

MATERIALS AND METHODS

Materials

RMP was provided by M/s. Sandoz Pharmaceuticals Ltd., Mumbai, as a kind gift sample. The phospholipid (Lipoid S-75) sample was kindly provided by Lipoid Ludwigshafen, Germany. Dichloromethane and other chemicals were obtained from Loba Chemie, Mumbai, India. Ammonium acetate was purchased from HiMedia, India. Methanol was purchased from Sigma Aldrich, Mumbai, India. All other chemicals were of analytical grade.

Preparation of SDRPLs

Three different batches of SDRPL varying drug to phospholipid ratio were prepared by spray drying (JISL Mumbai India with high-performance cyclone) a solution of RMP and PL (1:2, 1:1 and 2:1) (drug to phospholipid ratio) in dichloromethane. The feed solution was passed through a stainless steel 0.7 mm diameter atomizing nozzle via a peristaltic pump at a flow rate of 4 mL/min (pump rate 12%). The inlet temperature and outlet temperatures were set at 80 ± 2°C (primary drying step) and 55 ± 3°C (secondary drying step), respectively, with an aspirator rate of 90%. The resultant lipospheres were blown through a high-performance cyclone separator and collected in the sample container. Powder formulation was stored in glass vials sealed with parafilm at room temperature.

Drug Content and Encapsulation Efficiency

RMP content and encapsulation efficiency in the SDRPL formulation was determined using liquid chromatography-mass spectrometry (LCMS) (Thermo Scientific, LTQ XL, Germany). Accurately weighed samples of the microparticles were dissolved in 10 ml of methanol followed by centrifugation for 10 min at 10,000 rpm. Subsequently, 1 ml of aliquot was taken from supernatant and analyzed using validated LCMS method. For this analysis, methanol and ammonium acetate buffer system was used in the ratio of 70:30. The column used for chromatographic separation was Phenomenex C_{18} column (250 mm × 4.6 mm, 5 μm) and flow rate was 1 mL/min at ambient temperature. The detection wavelength was 475 nm, and injection volume was 20 μl. Calculations were carried out using the equations shown below:

$$\%\,\text{Drug content} = \frac{\text{Drug in lipospheres}}{\text{Mass of lipospheres}} \times 100 \quad (1)$$

$$\%\,\text{EE} = \frac{\text{Actual drug loading}}{\text{Theoretical drug loading}} \times 100 \quad (2)$$

Solubility Study of SDRPL

The thermodynamic solubility of RMP and SDRPLs was individually studied by adding an excess amount into distilled water in sealed glass vials at 25°C and shaken in shaker water bath (EQUITRON®, Mumbai, India) for 1 h. The obtained dispersion was centrifuged at 1200 rpm for 5 min and analyzed the samples by LCMS (Thermo Scientific, LTQ XL, Germany) as previously described. All experiments were carried out in triplicate.

Thermal Analysis

The thermodynamic behavior of RMP, phospholipid, physical mixture, and SDRPL formulation was studied by differential scanning calorimetry (DSC) in Mettler Toledo DSC (821e, Switzerland) equipped with Mettler Stare system. Samples of between 3 and 5 mg were weighed in aluminum pans and hermetically sealed for analysis. For this purpose, samples were heated from 25 to 250°C using a heating rate of 10°C/min. All experiments were run under a nitrogen gas flow set at 50 ml/min. Then, phase transition temperature and the melting point (Tm) of all the samples were determined.

Crystallographic Studies

Powder X-ray diffraction (PXRD) patterns of RMP, phospholipid, physical mixture, and SDRPL formulation were acquired on an X-ray diffractometer (Bruker AXS System D8, Germany) employing Cu κ-alpha radiation (tube operated at 35 kV, 20 mA) at room temperature. Data was collected over an angular range from 2° to 40° at a step rate of 0.01 2θ scale.

Hot-Stage Cross-Polarizing Light Microscopy

The phase transitions of RMP and SDRPL formulations were observed under a cross-polarizing light hot-stage microscope (HSM) (Leitz 1350, Leica, Germany) equipped with a 35-mm camera (Leica MPS 52) for the presence and/or absence of birefringence along with the melting behavior of the samples. Powder samples were mounted on a microscope slide, placed in the sample chamber and heated from 25 to 300°C at 5°C/min heating rate.

Surface Morphology

The particle surface morphology was studied by scanning electron microscopy (SEM) in a Hitachi S-800 microscope (Tokyo, Japan). The samples were placed on aluminum stubs and coated with a thin film of gold by Technics Hummer VI sputtering system at 10 AC mA for 3 min. The samples were scanned by an electron beam of 20 kV acceleration potential, at a working distance of 30 mm. The morphological structure of the drug-encapsulated lipopsheres was investigated by transmission electron microscopy (TEM) using TECNAI G^4 microscope with an accelerating voltage of 200 kV. For the TEM analysis, carbon-coated copper TEM grids, were used.

In vitro Antimycobacterial Activity

Test Strain

The antimycobacterial activity of SDRPL and RMP was tested on MTB H37Rv strain (Tuberculosis Research Centre, Chennai, India). Briefly, the bacteria were cultured in Middlebrook 7H9 liquid medium (HiMedia, India) supplemented with 10% albumin, dextrose, and catalase (ADC; HiMedia, India) to mid-log phase and then frozen in aliquots at −70°C until needed. Purity of culture was checked by Ziehl-Neelsen staining (HiMedia, India). Samples were dissolved in dimethyl sulphoxide (DMSO) and filter sterilized through 0.2-μm DMSO-Safe Acrodisc® syringe filters (PALL Life Sciences) before testing.

BACTEC 460TB Method

The BACTEC 460TB system (Becton Dickinson, USA) was employed to determine a growth index (GI) of the MTB. GI is the quantitative measure of $^{14}CO_2$ liberated by metabolism of ^{14}C-labeled substrate in a medium and expressed in numbers on a scale from 0 to 999. Briefly, 0.1 ml of samples were transferred to 12B BACTEC vials, in duplicate for each sample/drug concentration, unless mentioned otherwise, and incubated at 37°C in 5% CO_2 atm. GI was calculated daily under aerobic condition until in 1:100 controls and a value greater than 30 was obtained. In order to determine the percent inhibition, undiluted control reading was used. Appropriate positive and negative controls were also included in the calculation. The growth inhibition was expressed as a ratio of GI of drug to the respective control vial. The percent growth inhibition was calculated for each drug concentration (24,25).

In Vivo Oral Bioavailability Study

Chromatographic Condition

The plasma RMP was quantified by LCMS (Thermo Scientific, LTQ XL, Germany) with Phenomenex C18 column (250 mm × 4.6 mm, 5 μm). The optimized mobile phase is composed of a mixture of ammonium acetate buffer (2 mM) and acetonitrile in 30:70 proportions. The flow rate was maintained at 1 mL/min, and the samples were analyzed at room temperature.

Rifampicin Extraction and Sample Preparation

To a 200-μL rat plasma sample, 500 μL of methanol was added to extract the RMP. After vortex mixing (60 s), samples were centrifuged at 10,000 rpm for 10 min. Subsequently, 20 μL supernatant was taken and analyzed by LCMS (26).

Pharmacokinetic Studies of RMP and SDRPL

To carry out the pharmacokinetic studies, all the animal experiment protocols were approved by the Institutional Animal Ethics Committee (IAEC No. 108/1999/CPCSEA) first and then animals studies were performed in accordance with the CPCSEA (Committee for the Purpose of Control and Supervision of Experimentation on Animals) guidelines and maintained in an air-conditioned room (25 ± 2°C) with a 12-h light/12-h dark cycle. To perform the pharmacokinetic study, one batch of SDRPL formulation (1:1) was chosen based on the physical characteristics. Food and water were provided *ad libitum* to all the animals. Male albino Sprague Dawley rats (150–200 g) were divided into two groups ($n = 6$/group/time point), one group for RMP administration (15 mg/kg dose) and the other for SDRPL administration (dose equivalent to 15 mg/kg of RMP) with the help of an oral gavage. Blood samples were collected from the retro-orbital Plexus under light ether anesthesia at various time points into heparinized micro-centrifuge vials. Then, blood samples were centrifuged at 10,000 rpm for 10 min and analyzed by LCMS. Noscapine was the internal standard employed in the estimation.

Statistical Analysis

The results are expressed as mean ± S.D. Analysis was carried out using a statistical package program (GraphPad Prism 5 for Windows).

RESULTS

Drug Content and Encapsulation Efficiency

SDRPL formulations were prepared using different ratios of phospholipid and drug. It was found that phospholipid: drug ratio significantly affected the percent drug content of the formulations. The encapsulation efficiency increased with decrease in drug to phospholipid ratio. The drug content and encapsulation efficiency were found to be in the range of 41.52 ± 4 to 53 ± 4 (% *w*/*w*) and 73 ± 6 to 89 ± 4 (% *w*/*w*), respectively.

Solubility Study

Solubility of RMP and SDRPL formulations were determined in distilled water at 25°C. There was a significant increase ($p < 0.001$) in the solubility of SDRPL (2:1), 360 ± 12 *versus* 110.05 ± 15 μg/ml, and SDRPL (1:1) 310.12 ± 20 *versus* 110.05 ± 15 μg/ml in comparison to RMP. This improvement in solubility can be attributed to the

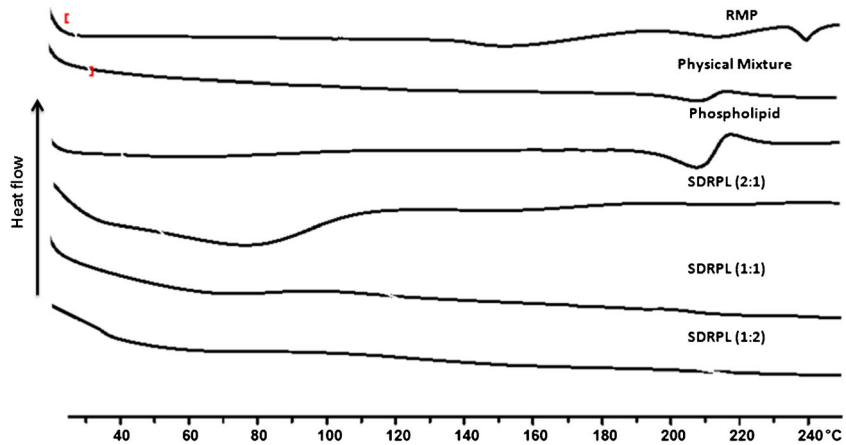

Fig. 1. DSC thermograms of RMP, physical mixture, and co-spray dried formulations

amorphous form of the SDRPL along with the solubilizing and surfactant effect of the phospholipid (27–29).

Thermal Analysis

The DSC thermograms of RMP *versus* SDRPL formulations are presented in Fig. 1. Pure RMP exhibited a small narrow endothermic phase transition peak, with onset temperature at d~190°C. The melting of crystalline RMP is similar to that reported in the literature (6,7). This order-to-disorder endothermic peak can be attributed to the melting process. These observations are in good agreement with previous reports on RMP, confirming its crystalline nature. Thermogram of phospholipid exhibited two distinct endotherms. The first endotherm was mild at 145–150°C suggesting movements of hot polar part of the phospholipid molecule. The second sharp endotherm peak at 230°C could be formed owing to the phase transition, from a gel-like to a liquid-crystal state, and perhaps due to melting of the carbon chain in the phospholipid or isomeric or crystal changes. Interestingly, DSC thermal analysis of SDRPL did not exhibit the RMP melting peak, suggesting a loss of crystallinity into a non-crystalline form (likely amorphous).

Crystallographic Analysis

Diffractograms of pure RMP and SDRPL formulations are presented in Fig. 2. RMP revealed sharp and narrow diffraction peaks at 11°, 13.5°, 16° and 20° 2θ scale, which is characteristic of a high degree of long-range molecular order (i.e., crystallinity). In the physical mixture, the diffraction peaks diminished to a certain extent. Contrastingly, in the diffractograms of SDRPL formulations, there was complete disappearance of sharp peaks, indicating loss in the crystalline nature of RMP. The loss of crystallinity of RMP following spray drying could be due to free

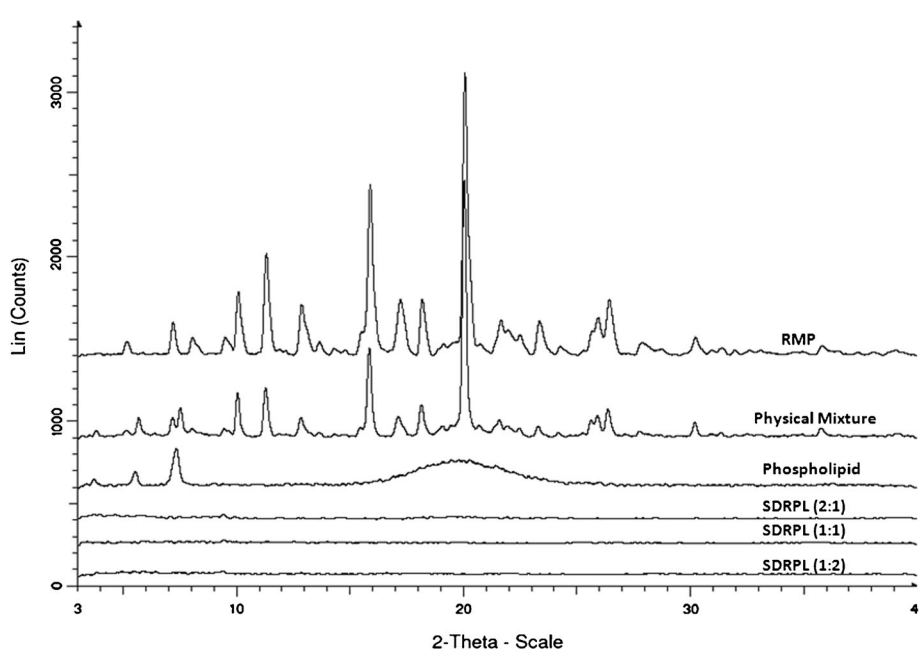

Fig. 2. PXRD diffractograms of RMP, physical mixture, and SDRPL

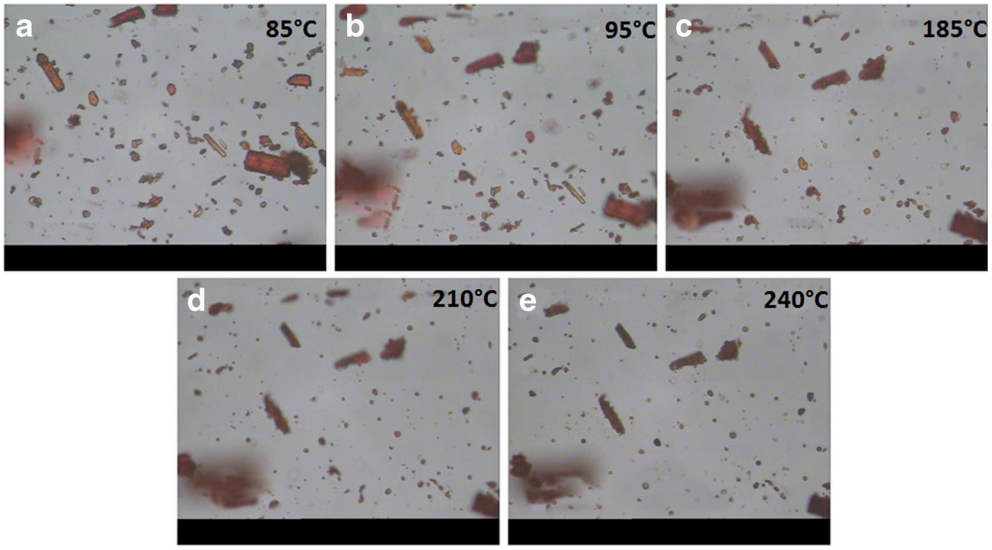

Fig. 3. HSM micrographs of pure RMP in ordinary light (**a–e**)

dispersion in the phospholipid matrix. This result, along with that of the thermal analysis, confirms conversion of drug into an amorphous state in the SDRPL formulation.

HSM

To examine the phase transitions of pure RMP, cross-polarized light optical microscope analysis was performed at a heating scan rate of 5°C/min. Under cross polarizer at room temperature, RMP exhibited crystal forms as shown in Fig. 3a–e. The onset temperature coincided with its melting recorded by DSC. Unsurprisingly, SDRPL formulations exhibited softening behavior, which is a characteristic feature of amorphous materials (Fig. 4a–e). The softening of the lipospheres started at the temperature ~102°C. Nominal birefringence of RMP was detected, which agrees with the PXRD diffractograms (Fig. 5a–e). The birefringence of pure RMP began diminishing with an increase in temperature. As expected for non-crystalline amorphous materials, the lipospheres formulation lacked birefringence, as displayed by the dark images (Fig. 6a–e). This was in a good agreement with the DSC thermal analysis findings and PXRD results. Blue arrow shows the softening of the lipospheres and birefringence of RMP, respectively.

Surface Morphology

The particle and surface morphology of RMP and SRDPL formulations were visualized and analyzed by SEM. The micrographs are presented in Fig. 7. RMP exhibited rod and columnar non-spherical morphology (Fig. 7a) (6). The lipospheres formulation at 1:1 ratio presented spherical particles with a smooth surface (Fig. 7b). On the contrary, the 2:1 and 1:2 ratios exhibited a little and great degree of aggregation as observed in

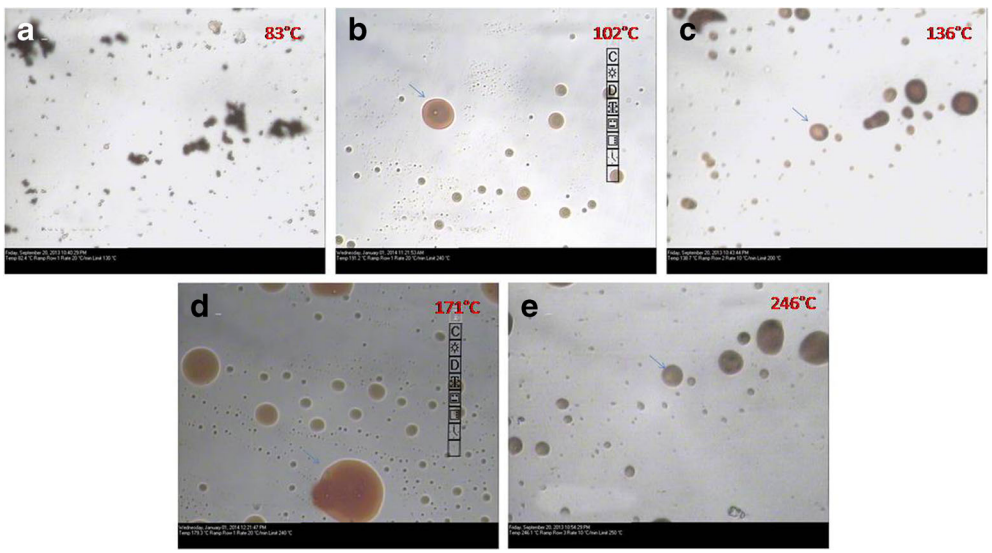

Fig. 4. HSM micrographs of SDRPL formulation in ordinary light (**a–e**)

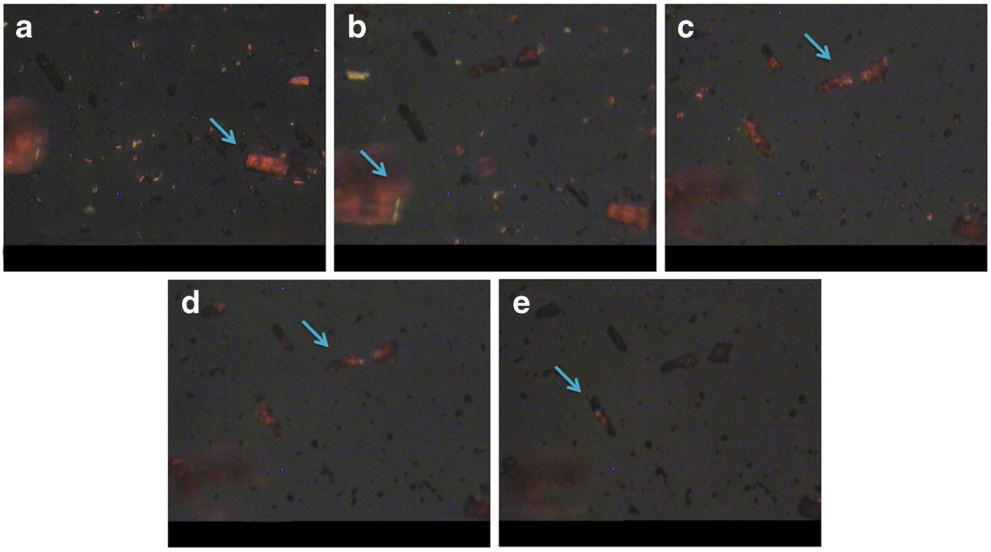

Fig. 5. HSM micrographs of pure RMP in cross polarized light (**a–e**)

Fig. 7c, d, respectively. This aggregation could be due to the presence of large amount of phospholipid in the formulation. Particles of all the liposphere formulations appear smaller than that of RMP. The former particles were spherical with a relatively smooth surface (30).

Transmission Electron Microscopy Analysis

TEM is employed for visualizing the surface morphology and size of the drug encapsulated lipospheres in water at room temperature. TEM analysis is ultimate for quantitatively visualizing the surface texture of the substance. TEM image of lipospheres is shown in Fig. 7e, wherein nanosized particles with average size of 231–250 nm were observed. These results suggest that phospholipids may serve as efficient delivery carriers for hydrophobic drugs.

In Vitro Antimycobacterial Activity

Two SDRPL formulations (1:1 and 2:1 proportions of drug to lipid) were selected based on surface morphology and ease of preparation and tested for antimycobacterial activity. Both the formulations exhibited enhanced efficacy *in vitro* in MTB H37Rv strain. DMSO was employed as the solubilizing agent and its possible inhibitory effect on MTB growth was considered, as well. There was a significant difference ($p < 0.001$) between minimum inhibitory concentration (MIC) values of RMP and SDRPL formulations against MTB, and it was found to be 0.025 (31) and 0.010 μg/ml, respectively. Thus, lipospheres formulation exhibited an enhanced antimycobacterial activity. This enhancement can be explained by an increase in surface area and stability of RMP and a potential solubi-

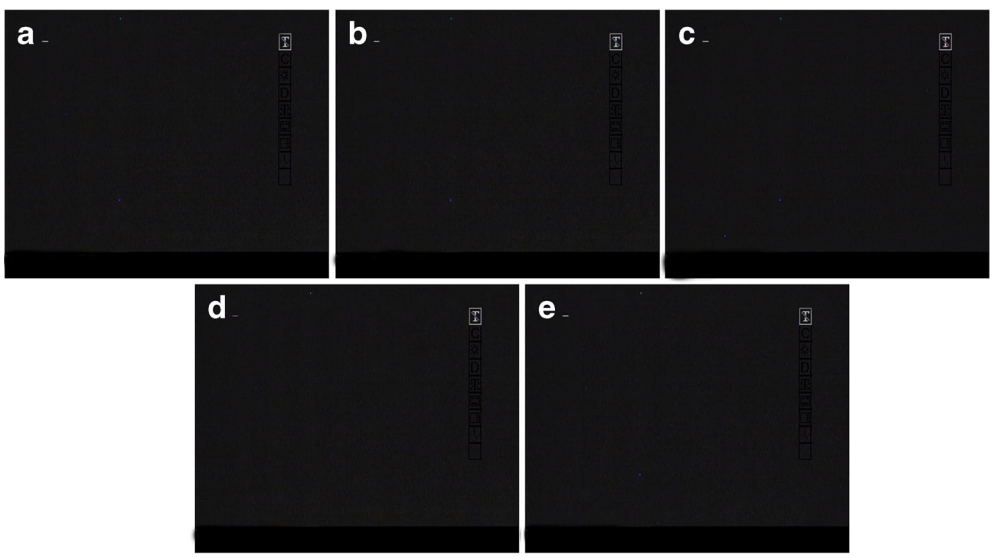

Fig. 6. HSM micrographs of SDRPL in cross polarized light (**a–e**)

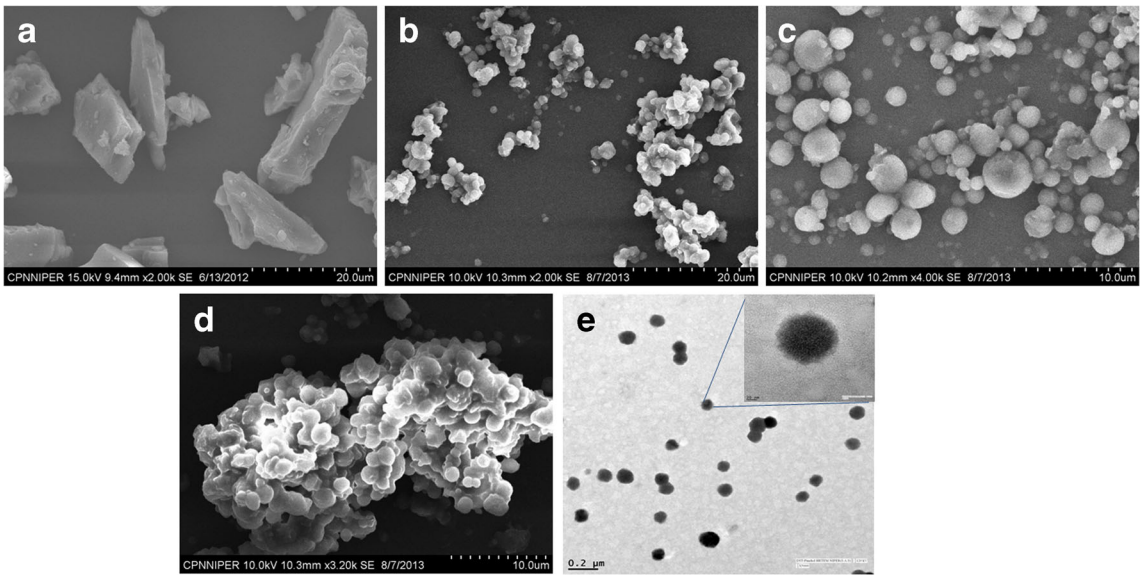

Fig. 7. SEM and TEM images of micrographs of pure RMP and SDRPL (**a–e**)

lizing effect of phospholipid. This is the first time that activity of a liposphere formulation of RMP has been reported.

In Vivo Oral Bioavailability Study

Figure 8 presents the plasma concentration *versus* time plots of RMP (15 mg/kg) and SDRPL formulation (equivalent to 15 mg/kg of RMP) after oral administration in SD rats. The lipospheres formulation exhibited increased C_{max} (109.92 ± 25 *versus* 54.31 ± 18 μg/ml) and faster T_{max} (2 *versus* 4 h) in comparison to pure RMP. Similarly, the area under the curve ($AUC_{0-\infty}$) value was 406.92 ± 18 *versus* 147.72 ± 15μgh/L in the lipospheres and RMP, respectively. Thus, a 275% increase was observed in the relative oral bioavailability of RMP in the liposphere formulation. Pharmacokinetic study data is compiled in Table I.

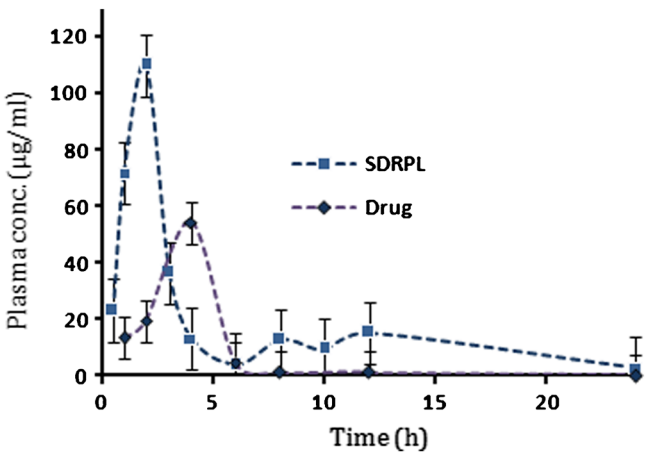

Fig. 8. Plot of plasma conc. *versus* time profile of RMP and SDRPL

RMP is a potential substrate for P-glycoprotein (P-gp) efflux (32) since P-gp substrates are cationic, hydrophobic molecules with at least two planar rings and molecular weights of 400–1500. Due to P-gp efflux action, RMP bioavailability is limited. This enhanced bioavailability can be explained by (1) the formation of self-assembled micelles of phospholipid lipospheres. The micelles increased the solubility and prevented the degradation of RMP in the gastrointestinal tract resulting in enhanced bioavailability by modifying the cell fluidity (33). In addition to this, micellar system bypass the P-gp efflux since transportation occurs through receptor-mediated endocytosis in comparison to diffusion for free drug into the cell (34,35).

(2) RMP is a potent enzyme inducer and induces its own metabolism which could decrease its bioavailability and efficacy (36). Addition into phospholipid matrix could limit its own metabolism, thereby increasing oral bioavailability. However, the reason for enhanced bioavailability via this mechanism is under investigation.

Table I. Pharmacokinetic Studies Data After Oral Administration of RMP and SDRPL to Rats

PK parameters	RMP	SDRPL
C_{max} (μg/mL)[a]	54.31 ± 18	109.92 ± 25***
T_{max} (h)[b]	4 ± 0.5	2 ± 1
$t_{1/2}$ (h)[c]	3.85 ± 0.5	7.11 ± 2***
MRT (h)[d]	1.53 ± 2	8.80 ± 3***
$AUC_{0-\infty}$ (μg h/mL)[e]	147.72 ± 15	406.92 ± 18***

Values are expressed as mean ± SD ($n = 6$)
***$p < 0.001$ shows significant difference from RMP
[a] C_{max}, maximum plasma concentration
[b] T_{max}, time when maximum plasma concentration is reached
[c] $t_{1/2}$, elimination half-life
[d] MRT, mean residence time
[e] $AUC_{0-\infty}$, area under the curve

CONCLUSIONS

In the present study, we reported microscale RMP lipospheres, SDRPL, for oral delivery. The particle and surface morphologies of RMP and SDRPL were studied by SEM. DSC and PXRD analyses were employed to study changes in physical characteristics after processing. HSM study further confirms the change from crystalline to amorphous form in the lipospheres formulation. TEM analysis showed nanosized particles with average size of 230–250 nm. *In vitro* antimycobacterial studies of SDRPL indicated its enhanced efficacy. It can be produced by an industrially viable, easily scalable technology with capability for modulating the size and functions. Thus, this can be concluded that novel SDRPL has exhibited increased antimycobacterial activity and oral bioavailability.

ACKNOWLEDGEMENTS

We wish to thank Mr. Vikas Grover and Mr. Rajdeo Kumar, CIL NIPER, for their kind technical help in LCMS and HPLC samples analysis, respectively. Technical support of Mr. Manish Kumar Verma and Mr. Sunil Kumar is duly acknowledged. We also wish to thank Mr. Rahul Mahajan, CPN NIPER, for SEM analysis. Authors are thankful to Mr. Vinod Kumar for TEM analysis.

COMPLIANCE WITH ETHICAL STANDARDS

Conflict of Interest The authors declare that they have no competing interests.

REFERENCES

1. Hirota K, Hasegawa T, Nakajima T, Inagawa H, Kohchi C, Soma G-I, *et al*. Delivery of rifampicin-PLGA microspheres into alveolar macrophages is promising for treatment of tuberculosis. J Control Release. 2010;142(3):339–46.
2. Onoshita T, Shimizu Y, Yamaya N, Miyazaki M, Yokoyama M, Fujiwara N, *et al*. The behavior of PLGA microspheres containing rifampicin in alveolar macrophages. Colloids Surf B. 2010;76(1):151–7.
3. Makino K, Nakajima T, Shikamura M, Ito F, Ando S, Kochi C, *et al*. Efficient intracellular delivery of rifampicin to alveolar macrophages using rifampicin-loaded PLGA microspheres: effects of molecular weight and composition of PLGA on release of rifampicin. Colloids Surf B. 2004;36(1):35–42.
4. Tomoda K, Makino K. Effects of lung surfactants on rifampicin release rate from monodisperse rifampicin-loaded PLGA microspheres. Colloids Surf B. 2007;55(1):115–24.
5. WHO. Global tuberculosis report 2014: World Health Organization; 2014.
6. Agrawal S, Ashokraj Y, Bharatam PV, Pillai O, Panchagnula R. Solid-state characterization of rifampicin samples and its biopharmaceutic relevance. Eur J Pharm Sci. 2004;22(2):127–44.
7. Bhise SB, More AB, Malayandi R. Formulation and in vitro evaluation of rifampicin loaded porous microspheres. Sci Pharm. 2009;78(2):291–302.
8. Agrawal S, Panchagnula R. Dissolution test as a surrogate for quality evaluation of rifampicin containing fixed dose combination formulations. Int J Pharm. 2004;287(1):97–112.
9. Lindenberg M, Kopp S, Dressman JB. Classification of orally administered drugs on the world health organization model list of essential medicines according to the biopharmaceutics classification system. Eur J Pharm Biopharm. 2004;58(2):265–78.
10. Singh C, Bhatt TD, Gill MS, Suresh S. Novel rifampicin-phospholipid complex for tubercular therapy: synthesis, physicochemical characterization and in-vivo evaluation. Int J Pharm. 2014;460(1):220–7.
11. Wong S, Kellaway I, Murdan S. Enhancement of the dissolution rate and oral absorption of a poorly water soluble drug by formation of surfactant-containing microparticles. Int J Pharm. 2006;317(1):61–8.
12. Jahan R, Islam MS, Tanwir A, Chowdhury JA. In vitro dissolution study of atorvastatin binary solid dispersion. J Adv Pharm Technol Res. 2013;4(1):18.
13. Vasconcelos T, Sarmento B, Costa P. Solid dispersions as strategy to improve oral bioavailability of poor water soluble drugs. Drug Discov Today. 2007;12(23):1068–75.
14. Han S-F, Yao T-T, Zhang X-X, Gan L, Zhu C, Yu H-Z, *et al*. Lipid-based formulations to enhance oral bioavailability of the poorly water-soluble drug anethol trithione: effects of lipid composition and formulation. Int J Pharm. 2009;379(1):18–24.
15. He D, Deng P, Yang L, Tan Q, Liu J, Yang M, *et al*. Molecular encapsulation of rifampicin as an inclusion complex of hydroxypropyl-β-cyclodextrin: design; characterization and in vitro dissolution. Colloids Surf B. 2013;103:580–5.
16. Mu H, Holm R, Müllertz A. Lipid-based formulations for oral administration of poorly water-soluble drugs. Int J Pharm. 2013;453(1):215–24.
17. Chimote G, Banerjee R. Evaluation of antitubercular drug insertion into preformed dipalmitoylphosphatidylcholine monolayers. Colloids Surf B. 2008;62(2):258–64.
18. Yanyu X, Yunmei S, Zhipeng C, Qineng P. The preparation of silybin-phospholipid complex and the study on its pharmacokinetics in rats. Int J Pharm. 2006;307(1):77–82.
19. Maiti K, Mukherjee K, Gantait A, Saha BP, Mukherjee PK. Curcumin-phospholipid complex: preparation, therapeutic evaluation and pharmacokinetic study in rats. Int J Pharm. 2007;330(1):155–63.
20. Singh D, Rawat M, Semalty A, Semalty M. Rutin-phospholipid complex: an innovative technique in novel drug delivery system-NDDS. Curr Drug Deliv. 2012;9(3):305–14.
21. Hüsch J, Dutagaci B, Glaubitz C, Geppert T, Schneider G, Harms M, *et al*. Structural properties of so-called NSAID-phospholipid-complexes. Eur J Pharm Sci. 2011;44(1):103–16.
22. Elversson J, Millqvist-Fureby A, Alderborn G, Elofsson U. Droplet and particle size relationship and shell thickness of inhalable lactose particles during spray drying. J Pharm Sci. 2003;92(4):900–10.
23. Costantino HR, Andya JD, Nguyen PA, Dasovich N, Sweeney TD, Shire SJ, *et al*. Effect of mannitol crystallization on the stability and aerosol performance of a spray-dried pharmaceutical protein, recombinant humanized anti-IgE monoclonal antibody. J Pharm Sci. 1998;87(11):1406–11.
24. Huang T-S, Tu H-Z, Lee SS-J, Huang W-K, Liu Y-C. Antimicrobial susceptibility testing of Mycobacterium tuberculosis to first-line drugs: comparisons of the MGIT 960 and BACTEC 460 systems. Ann Clin Lab Sci. 2002;32(2):142–7.
25. Jagannath C, Reddy MV, Kailasam S, O'Sullivan J, Gangadharam P. Chemotherapeutic activity of clofazimine and its analogues against Mycobacterium tuberculosis. In vitro, intracellular, and in vivo studies. Am J Respir Crit Care Med. 1995;151(4):1083–6.
26. Patil JS, Suresh S, Sureshbabu AR, Rajesh MS. Development and validation of liquid chromatography-mass spectrometry method for the estimation of rifampicin in plasma. Indian J Pharm Sci. 2011;73(5):558–63. doi:10.4103/0250-474X.99014.
27. Singh D, Rawat MS, Semalty A, Semalty M. Quercetin-phospholipid complex: an amorphous pharmaceutical system in herbal drug delivery. Curr Drug Discov Technol. 2012;9(1):17–24.
28. Rawat DS, Thakur BK, Semalty M, Semalty A, Badoni P, Rawat MSM. Baicalein-phospholipid complex: a novel drug delivery technology for phytotherapeutics. Curr Drug Discov Technol. 2013;10(3):224–32.
29. Semalty A, Semalty M, Singh D, Rawat M. Development and physicochemical evaluation of pharmacosomes of diclofenac. Acta Pharma. 2009;59(3):335–44.

30. Wu X, Hayes Jr D, Zwischenberger JB, Kuhn RJ, Mansour HM. Design and physicochemical characterization of advanced spray-dried tacrolimus multifunctional particles for inhalation. Drug Des Dev Ther. 2013;7:59.
31. Sung JC, Padilla DJ, Garcia-Contreras L, VerBerkmoes JL, Durbin D, Peloquin CA, *et al*. Formulation and pharmacokinetics of self-assembled rifampicin nanoparticle systems for pulmonary delivery. Pharm Res. 2009;26(8):1847–55.
32. Srivalli KMR, Lakshmi P. Overview of P-glycoprotein inhibitors: a rational outlook. Braz J Pharm Sci. 2012;48(3):353–67.
33. Kaur V, Garg T, Rath G, Goyal AK. Therapeutic potential of nanocarrier for overcoming to P-glycoprotein. J Drug Target. 2014;0:1–12.
34. Dabholkar RD, Sawant RM, Mongayt DA, Devarajan PV, Torchilin VP. Polyethylene glycol-phosphatidylethanolamine conjugate (PEG-PE)-based mixed micelles: some properties, loading with paclitaxel, and modulation of P-glycoprotein-mediated efflux. Int J Pharm. 2006;315(1):148–57.
35. Kobayashi T, Ishida T, Okada Y, Ise S, Harashima H, Kiwada H. Effect of transferrin receptor-targeted liposomal doxorubicin in P-glycoprotein-mediated drug resistant tumor cells. Int J Pharm. 2007;329(1):94–102.
36. Chen J, Raymond K. Roles of rifampicin in drug-drug interactions: underlying molecular mechanisms involving the nuclear pregnane X receptor. Ann Clin Microbiol Antimicrobiol. 2006;5(1):3.